

# Electrophysiological Analysis of Membrane Disruption by Bombinin and Its Isomer Using the Lipid Bilayer System

Yusuke Sekiya,<sup>†,||</sup> Keisuke Shimizu,<sup>†,||</sup> Yuki Kitahashi,<sup>‡</sup> Akifumi Ohyama,<sup>§</sup> Izuru Kawamura,<sup>‡,§,ⓑ</sup> and Ryuji Kawano<sup>\*,†,ⓑ</sup>

<sup>†</sup>Department of Biotechnology and Life Science, Tokyo University of Agriculture and Technology, 2-24-16 Naka-cho, Koganei, Tokyo 184-8588, Japan

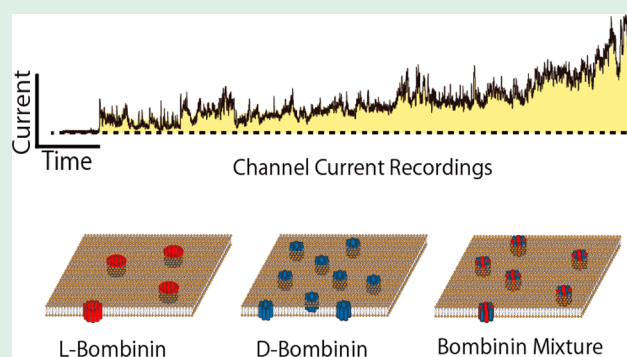
<sup>‡</sup>Graduate School of Engineering, Yokohama National University, Hodogaya-ku, Yokohama 240-8501, Japan

<sup>§</sup>Graduate School of Engineering Science, Yokohama National University, Hodogaya-ku, Yokohama 240-8501, Japan

## Supporting Information

**ABSTRACT:** Bombinin H2 and H4 are peptides isolated from the skin of the frog *Bombina variegata* that exhibit antimicrobial activity against *Leishmania* as well as bacteria. H4 is an isomer of H2 that has D-allo-Ile at position 2 from the N-terminus. Although H4 exhibits higher antimicrobial activity than that of H2, the molecular mechanism has remained unclear. In this study, we tried to reveal the molecular mechanism in terms of lipid membrane disruption through pore formation, using electrophysiological measurements. Based on our experiments, we estimated the pore-forming structure, pore size, and the kinetics in a bacteria model membrane. Stochastic analysis of the current data indicated that peptide isomerization enables us to accelerate the pore formation owing to the higher affinity between the peptide and lipid membrane. Additionally, the H2/H4 mixture was studied with <sup>31</sup>P NMR and cross-linking experiment with mass spectrometry. It was found that heterogeneous pore formation with H2 and H4 was indicated. This electrophysiological approach will likely be promising as a useful tool for analyzing the molecular mechanism of pore-forming peptides.

**KEYWORDS:** antimicrobial peptide, bombinin, isomer, electrophysiology, lipid bilayer, solid-state NMR



## INTRODUCTION

The isomerization of peptides constitutes an intriguing event of biosynthesis because of its unique capability of modifying the biochemical properties of the original peptide.<sup>1</sup> For example, one of the opiate peptides, dermorphin, secreted in the skin of the South America tree frog contains D-Ala at position 2 from the N-terminus.<sup>2</sup> This type of isomer exhibits higher binding affinity and selectivity to  $\mu$ -opiate receptors. Similarly, bombinin H, which is an antimicrobial peptide (AMP) isolated from skin secretions of the frog *Bombina variegata*, contains either L-Ile or D-allo-Ile at the position of the second amino acid from the N-terminus, as all L-peptide bombinin H2 (IIGPVLGLVG-SALGGLLKKI-NH<sub>2</sub>) or its diastereomer H4 (Figure 1a).<sup>3</sup> Several studies have reported that bombinin H4 showed higher antimicrobial activity than that of H2.<sup>4</sup> In particular, bombinins are potent candidates as medicine for *Leishmania*, which constitutes an infectious disease with a global incidence of 10 to 12 million people infected.<sup>5</sup> Bombinins can directly impact *Leishmania*, whereas only a few other AMPs have been known to exhibit leishmanicidal activity, the majority of which acts mainly on the insect stage of the parasite (promastigotes).<sup>6</sup> Although the bombinins are expected to function as unique AMPs upon

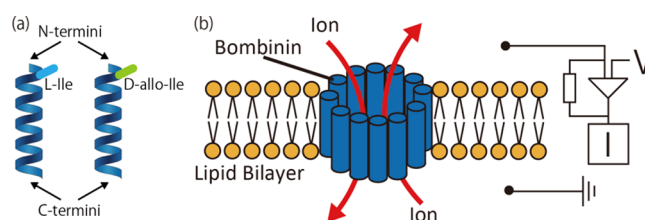


**Figure 1.** Schematic diagrams of L- and D-bombinins and their pore formation in the planar lipid bilayer system. (a) Schematic structure of bombinins H2 (left) and H4 (right). (b) Schematic diagram of the channel current measurement using a planar bilayer lipid membrane (pBLM).

isomerization even against *Leishmania*, the molecular mechanism of their activity remains under debate.

In this study, we hypothesize that the main activity of bombinins is probably due to the membrane disruption as indicated from several prior experiments.<sup>7,8</sup> Thus, we examined

**Received:** December 27, 2018

**Accepted:** February 20, 2019

**Published:** February 20, 2019

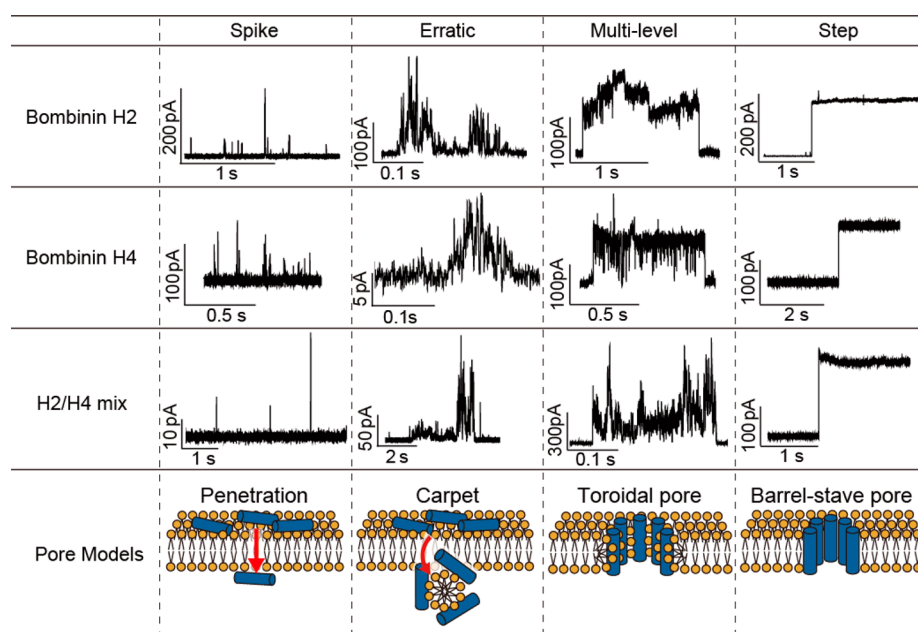


**Figure 2.** Classification of the channel current signals and possible models of the transmembrane structure of bombinins from among those previously proposed. The assignment between the current signals and pore-forming models has been proposed in our previous study (ref 22).

the pore-forming behavior of H2 and H4 using a planar bilayer lipid membrane (pBLM) as a model bacteria membrane (Figure 1b). The electrophysiological method of pBLM will likely be a useful tool for analyzing the molecular mechanism of pore-forming peptides in comparison to the conventional methods for membrane peptide analysis, which rely on spectroscopic or simulation study. We have previously proposed high-throughput pBLM formation by using a microfabricated device as shown in Figure S-1 (see the details in Methods).<sup>9–13</sup> Using this system, we have reported the pore-forming behavior of the AMP, magainin, and estimated the pore formation model using stochastic current analysis.<sup>14</sup> Based on our systematic method, in the current study, we attempt to reveal the pore-forming activity of bombinins H2 and H4 and their mixture at the molecular basis and discuss the relationship between the pore formation behavior and antimicrobial activity.

## RESULTS

**Signal Classification and Estimation of Pore-Forming Mechanisms.** Bombinin H2, H4, and the H2/H4 mixture were represented by the four different current signals in this measurement. We classified these signals as shown in Figure 2; the signals were defined as a step, multilevel, erratic, and spike. These, along with their possible pore-forming models from the literature,<sup>14–16</sup> are described as follows.

- (i) *Step signal*: a current jumps up orthogonally and maintains a plateau state. This signal can apply to a “barrel-stave” model<sup>17</sup> wherein transmembrane peptides are tightly assembled with each other and form a rigid circular pore.
- (ii) *Multilevel signal*: current shows fluctuation after jumping up and goes back to the initial state. This current may indicate a “toroidal” model<sup>18</sup> whereby transmembrane peptides form a pore with lipids. In this model, the size of the pore can change dynamically with or without the participation of the lipid between the monomers.
- (iii) *Erratic signal*: a current represents random increases with fluctuation. We assigned this signal to a “carpet” model.<sup>19</sup>

The carpet model has been described such that peptides bind parallel to the lipid bilayer surface, and after reaching sufficient coverage, they unwrap lipids as a peptide–lipid cluster from the membrane similar to a detergent. The random current behavior of the erratic signal would be caused by the random size of the cluster.

- (iv) *Spike signal*: a current suddenly raises up and then goes back to the baseline over a period of less than 20 ms, as we define here. This signal indicates an instantaneous membrane defect. We apply this signal to peptide permeation<sup>20</sup> through the membrane.

These pore-forming models of AMPs have been already proposed; we have attempted to apply these models to the different behaviors of the observed channel currents<sup>21</sup> and recently to assign the signals using magainin, alamethicin, and LK model peptides as toroidal/carpet, barrel-stave, and penetration model peptides.<sup>22</sup> We counted these signals from the initial signal until more than a hundred signals, as an index of pore stability of peptides. However, during this counting, the different signals sometimes overlapped at the same time. These signals reflect that several pores are formed in the lipid bilayer membrane, and the diameter is about 100  $\mu\text{m}$ . For example, spike signals were occasionally observed on the plateau region of the step signal, and we did not count the overlapped signals in this case. The ratio of the signal appearance is shown in Figure 3.

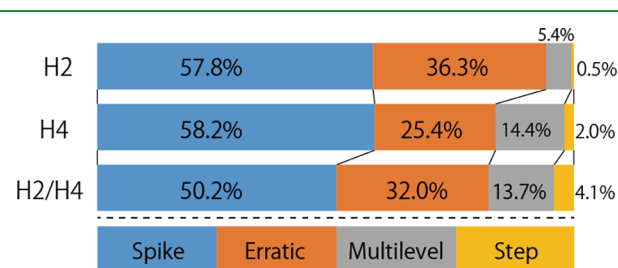


**Figure 3.** Ratio of appearance for each current signal ( $n > 200$  in each peptide).

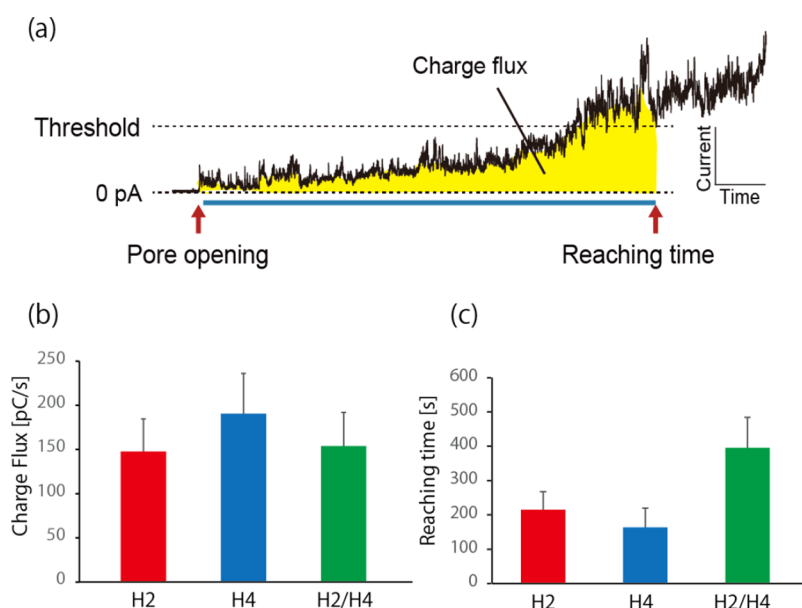


**Figure 4.** (a) Definition of the charge flux and the reaching time for analyzing the channel current recordings. The charge flux (b) and the current reaching time (c) for threshold current of 500 pA.

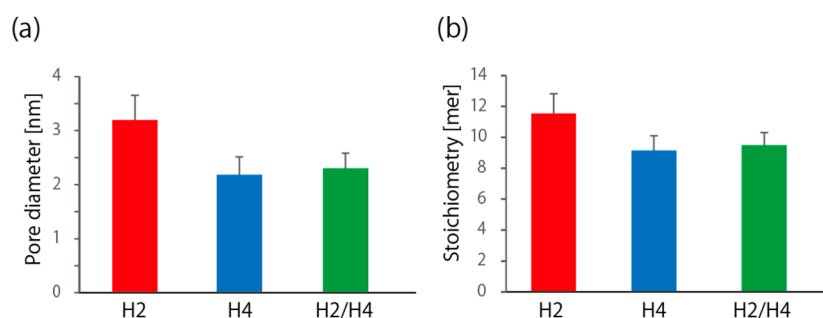


**Figure 5.** Pore diameter and stoichiometry of bombinins with a barrel-stave pore. (a) Pore diameter of each bombinin calculated from the Hille model. (b) Mathematical estimation of the stoichiometry (number of peptide monomers for forming the pore) using the pore diameters and the monomer size ( $n > 30$ ).

The ratio of spike signals was the highest in all three systems of H2, H4, and mixture, after which the order was as follows: the erratic > multilevel > step signal. This tendency is reflected in the pore formability of bombinins.<sup>22</sup> In terms of pore formability of the four models, we assume that the formality of stable pore which means to form a more cylindrical shape is spike < erratic < multilevel < step signal. Therefore, the result of the tendency of the ratio suggests that the capability of the stable pore formation would be energetically unfavorable in this condition. In addition, this estimation was conducted by counting the number of signals, resulting in counting a large amount of the spike and erratic signals. The appearance probability of these two signals was relatively high, whereas the duration was shorter than other signals. Therefore, we analyzed the duration time of the pore formation (Table S-1). As the result, the duration time of each signal was: spike < erratic < multilevel < step signal as the same order of pore stability. This fact suggested that the stable pore formation may strongly contribute to the membrane defect. Compared to H2 and H4, the step and multilevel signals in H4 were more than those in H2 as opposed to the erratic signals, suggesting that H4 may be likely to form a rigid pore. In addition, the mixture of H2/H4 showed a higher ratio of the step signals. This result implies the high possibility of rigid pore formation.

**Ion Leaking Activity and Kinetics of the Pore Formation.** The leaking experiment is normally performed to estimate the antimicrobial activity of membrane disruption. In the current study, we focused on the charge flux instead of the leaking experiment, which is the total amount of ion transportation through the pore.<sup>23</sup> Figure 4a shows the typical erratic signal and the method used to estimate the charge flux. The charge flux was defined as the average charge per unit time from the initial current increase to the threshold and never goes below the line, as presented in the yellow area in Figure 4a. In this estimation, the rapid current overflow for less than 10 s that may indicate the membrane rupture was not counted. Figure 4b shows the charge flux of H2, H4, and H2/H4 using the threshold of 500 pA. Although the value of H4 was slightly higher than that of others, the difference was not clear. Therefore, we checked the other threshold values of 100 and 1000 pA. The order of values was  $H4 \geq H2/H4 \geq H2$  in all threshold conditions (Figure S-2). The charge flux should reflect the activity of ionic leakage that will correspond to the ion permeability via the lipid membrane. In addition, the tendency of the total pore area would also be  $H4 \geq H2/H4 \geq H2$  if the ability of ion permeability per unit pore area per time (permeability/( $\text{nm}^2 \text{ s}$ )) of all bombinins is constant.

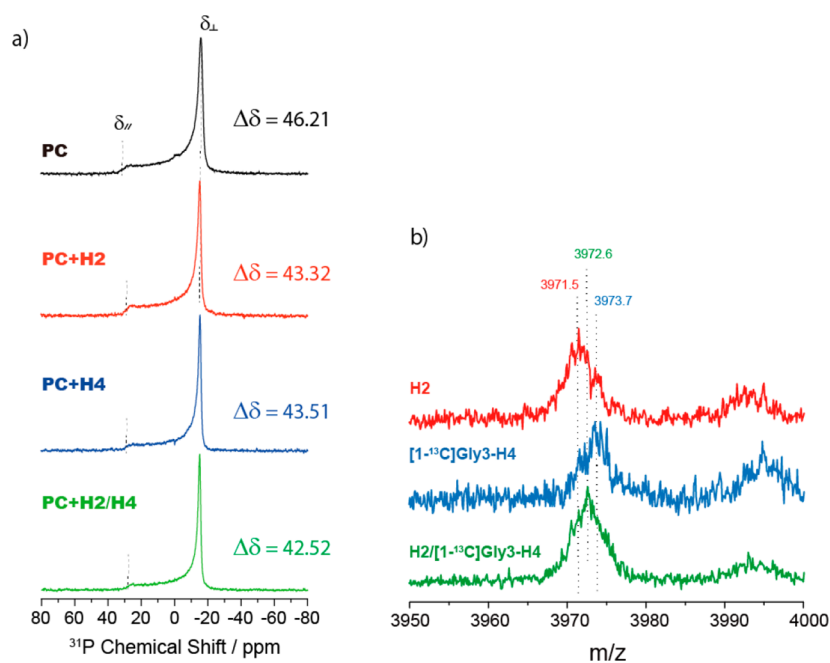


**Figure 6.** (a)  $^{31}\text{P}$  static solid-state NMR spectra of PC (black), PC-H2 (red), PC-H4 (blue), and PC-H2/H4 (green) at 30 °C.  $\Delta\delta = \delta_{\parallel} - \delta_{\perp}$ . (b) MALDI-TOF MS spectra of cross-linked H2 (red),  $[1-^{13}\text{C}]$ Gly3-H4 (blue), and the 1:1 mixture (green) in PE/PG using BS $^3$  linking reagent.

We initially considered that the charge flux may be the suitable parameter for reflecting the membrane dysfunction of antimicrobial peptides. However, if the pore formation is very slow even if the pore size is large, this type of mechanism may not show the higher microbial activity. Thus, we examined both the dynamics and kinetics of membrane disruption. The kinetics of the pore formation was analyzed by the time to over the threshold from the initial current appearance, termed “reaching time”. This time indicates the kinetics for generating membrane defects by the pore formation. Notably, the time in the H2/H4 mixture system was much slower than that in H2 or H4 systems. The time in H2 was slightly slower than that in the H4 system, as shown in Figure 4c.

**Pore Size and Stoichiometry of Bombinin H2, H4, and the H2/H4 Mixture.** The step signals will reflect the stable pore formation, as peptide monomers assemble to form fixed pores in a lipid membrane. We calculated the pore diameter using the amplitude of step currents and the Hille model.<sup>24</sup>

$$R = \left( l + \frac{\pi r}{2} \right) \frac{\rho}{\pi r^2} \quad (1)$$

where  $r$  is the pore radius;  $\rho$  is the resistivity of the buffered solution;  $l$  is the length of the pore (5 nm);<sup>25</sup> and  $R$  is the resistivity of the pore.  $R$  is calculated as  $V/I$ , where  $I$  is the current through the pore and  $V$  is the applied voltage between two chambers (100 mV). The pore diameters on each bombinin are presented in Figure 5a. The diameters of H2, H4, and H2/H4 pores were  $3.2 \pm 0.5$ ,  $2.2 \pm 0.3$ , and  $2.3 \pm 0.3$  nm, respectively; the order of pore diameter was  $\text{H2} > \text{H2/H4} \approx \text{H4}$  in this calculation.

Next, we estimated the number of assembling monomers from the step signals. This signal would reflect a barrel-stave pore formation as mentioned above. Because a barrel-stave pore is a cylindrical pore that consists of assembling monomers at the periphery, we mathematically estimated the stoichiometry using a multimeric model.<sup>14</sup>

$$d = a \left( \frac{1}{\sin(\pi/n)} - 1 \right) \quad (2)$$

where  $d$  is the pore diameter;  $a$  is the width of a peptide monomer from the PDB ( $a = 1.1$  nm); and  $n$  is the number of assembling monomers. Figure 5b shows the number of monomers: H2, H4, and H2/H4 were  $11.5 \pm 1.3$ ,  $9.1 \pm 1.0$ , and  $9.5 \pm 0.8$  molecules, and the order was  $\text{H2} > \text{H2/H4} \approx \text{H4}$  in this estimation.

**Estimation of Heterogeneity of Forming Pores Using  $^{31}\text{P}$  NMR and Cross-Linking Experiment.** To estimate the heterogeneity of the formed pore in the H2/H4 system, we conducted a  $^{31}\text{P}$  solid-state NMR and cross-linking experiment.<sup>26</sup> The chemical shift anisotropy ( $\Delta\delta/\text{ppm}$ ), which reflects the dynamics and orientation of phospholipids, showed  $\text{H2/H4} < \text{H2} \approx \text{H4}$  (Figure 6a), suggesting the heterogeneous pore formation. If the homogeneous pore formation occurs in the H2/H4 system, that value would show the similar value of H2 and H4. In addition, we attempted to reveal the heterogeneity based on more direct evidence using cross-linking experiment. In this method, we synthesized and used a  $^{13}\text{C}$ -labeled H4 monomer. The two monomers in the pore reconstituted in liposomes were cross-linked using *N*-hydroxysulfo-succinimide (NHS) ester in short reaction time, and then we carefully checked the weight of the dimer using matrix-assisted laser desorption ionization-time-of-flight mass spectrometry (MALDI-TOF MS). As the results, the peak from the H2/H4 system was in between H2 and H4 systems (Figure 6b), suggesting the heterogeneous pore formation in the mixed system.

## DISCUSSION

In the previous study of the antimicrobial activities of bombinins, the activity estimated from the minimum inhibitory concentration (MIC) of H4 was higher than that of H2 to Gram-negative bacteria.<sup>4</sup> Several mechanisms for these activities are generally considered to exist such as chemical enzyme inhibition

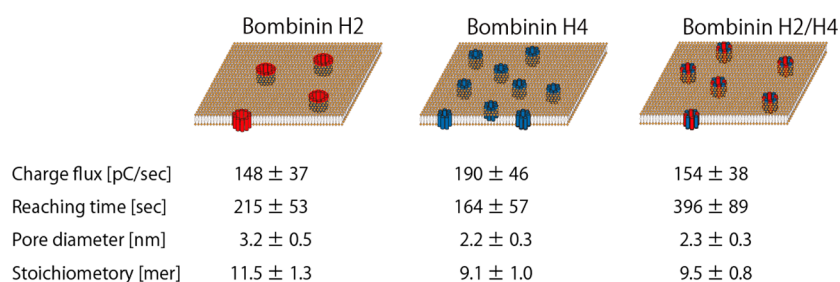


**Figure 7.** Proposed models for the pore formation of bombinin H2 and H4 in this study and summary of all analyzed data of the pore formation activities.

in the metabolic pathway or physical membrane disruption. According to previous experiments on bombinins, the measurements of fluorescein leakage through the lipid membrane by bombinins using living cells or liposomes show  $H4 > H2$ .<sup>7</sup> These leak experiments indicate that the pore formation of bombinins into the lipid membrane constitute the important factor of antimicrobial activity and that the activity of H4 is much higher than that of H2.<sup>7</sup>

Several experiments using circular dichroism (CD), Fourier transform infrared spectroscopy (FTIR), electron microscopy, and surface plasmon resonance (SPR) measurements have attempted to reveal the molecular mechanism of membrane disruption.<sup>4,6</sup> Through these experiments, two important facts were exhibited: (1) the  $\alpha$ -helicity which is strongly related with the membrane disruption of bombinins was  $H2 \approx H4$  based on CD and FTIR measurements and (2) the binding affinity to the lipid membrane was  $H4 > H2$  according to SPR measurements using a *Leishmania* model membrane (PE/PC/PI/PS/erg). The  $\alpha$ -helicity did not affect the antimicrobial activity in this case, whereas the  $\alpha$ -helicity of AMPs is generally related to the antimicrobial activity. In comparison, the lower binding affinity of H2 than H4 was probably due to its reduced hydrophobicity. Molecular dynamics simulation of the hydrated *Leishmania* membrane–peptide systems showed that the *D*-allo-Ile in bombinin H4 plays the role of a hydrophobic anchor in the membrane.<sup>26</sup> Other structural variances between H2 and H4 have been reported using nuclear magnetic resonance,<sup>27</sup> electron microscopy,<sup>6</sup> and molecular dynamic simulation of dissolved peptides;<sup>8</sup> however, the critical explanation regarding the molecular basis of membrane disruption was still required, even in the H2/H4 mixtures. H2/H4 mixtures would play an important role in nature because H4 is isomerized and coexists with H2 as the mixture.<sup>28</sup>

In our electrophysiological measurements, three notable results were obtained: (1) ion permeability from the charge flux analysis, (2) pore-forming kinetics from the reaching time measurements, and (3) pore size estimation from the step current.

- (1) *Ion permeability,  $H4 > H2/H4 \geq H2$* : This order is consistent with the results of the leak experiment using cells or liposomes in the previous reports. It is reasonable because the permeability and leak experiments should reflect similar phenomena. The values of H2 and H2/H4 were close in this estimation.
- (2) *Pore-forming kinetics,  $H4 \geq H2 > H2/H4$* : In this estimation, the kinetics of the H2/H4 mixture was lower than that of H2 or H4, whereas the values of H2 and H4 were close to each other.
- (3) *Pore size,  $H2 \geq H2/H4 \approx H4$* : This order is consistent with the  $\alpha$ -helicity. Reasonably, the  $\alpha$ -helicity is strongly

related to the transmembrane structure and pore formation.

These values are listed in Figure 7. Summarizing these data, we consider the pore-forming model of each bombinin as also shown in Figure 7. Bombinin H2 forms relatively large pores, and bombinin H4 rapidly forms smaller pores. In the case of their mixture, the kinetics of pore formation is the lowest with medium-sized pores. Although the insertion of a *D*-amino acid in the second position of the bombinin sequence should render it difficult to form the large pore with a barrel-stave shape, it would enhance the formation of the membrane defect owing to the high binding affinity to the membrane.

Another question is that the formed pore of the H2/H4 system is homogeneous or heterogeneous, whereas the electrophysiological results imply the heterogeneity. The binding between H2 and H4 may be stronger than that between the homogeneous states of H2–H2 or H4–H4 because the kinetics of the mixture decreased compared to the homogeneous state. Other experimental results using the solid-state <sup>31</sup>P NMR and the cross-linking experiments indicated the heterogeneous pore formation. Considering these facts, although the H4 has the highest membrane disruption capability, the pore-forming kinetics is regulated without reducing the pore-forming ability in the case of an H2/H4 mixture. The living system may regulate the antimicrobial activity using the isomerization of bombinin.

## CONCLUSIONS

In summary, we estimated the pore-forming activity of bombinin H2, H4, and their mixtures with the channel current measurement using the pBLM system with the model bacterial membrane. The model membrane allows us to use the pure lipid contents. The four different current signals were observed and were applied to pore formation models of AMPs that have been already proposed. Then, the probability of the appearance of the four current types was analyzed, estimating the pore-forming activity of each peptide. Next, we examined the following three behaviors: (1) ion permeability from the charge flux analysis, (2) pore-forming kinetics from the reaching time measurements, and (3) pore size estimation from the step current. From the results of the analysis, we concluded and proposed the pore-forming models for bombinin H2, H4, and H2/H4 mixtures to the bacterial model membrane. These models well explain the antimicrobial activity on a molecular basis. Our systematic electrophysiological measurements and the signal classification analysis will contribute useful insights into the molecular mechanism of antimicrobial activities for transmembrane peptides and/or other transmembrane molecules such as a synthetic channel.<sup>29,30</sup> In addition, the *D*-amino acids can be used for regulating the properties of *L*-peptides at the molecular

level, suggesting that it would be a strong tool for extensive biomaterials in nanoscience and medical applications.

## EXPERIMENTAL SECTION

**Chemicals.** In this study, the reagents were obtained as follows: 1,2-dioleoyl-*sn*-glycero-3-phospho-(1'-*rac*-glycerol) (DOPG; Avanti Polar Lipids); 1,2-dioleoyl-*sn*-glycero-3-phosphoethanolamine (DOPE; Avanti, Polar Lipids); *n*-decane (Wako Pure Chemical Industries, Ltd.); 3-morpholinopropane-1-sulfonic acid (MOPS, Nacalai Tesque); and KCl (Nacalai Tesque). Buffered electrolyte solutions were prepared from ultrapure water, which was obtained from a Milli-Q system (Millipore). Bombinin H2 and H4 were synthesized by microwave-assisted solid-phase peptide chemistry using an Initiator+Alstra peptide synthesizer (Biotage) and purified by reverse-phase HPLC on a C-18 ODS column (Purity >90%, TOF-Mass data are shown in Figure S-3) and dissolved at a concentration of 1 mg mL<sup>-1</sup> in ultrapure water and stored at -20 °C.<sup>31</sup> For use, samples were diluted to 100 μM using a buffered electrolyte solution and stored at 4 °C.

**Preparation of a High-Throughput pBLM Device.** The multichannel device was fabricated by machining a 6.0 mm thick, 10 × 10 mm poly(methyl methacrylate) (PMMA) plate (Mitsubishi Rayon) using a CAD/CAM 3-D modeling machine (MM-100, Modia Systems) (Figures S-1a and S-1b). A polymeric film made of parylene C (polychloro-*p*-xylylene) with a thickness of 5 μm was patterned as a single pore (100 μm in diameter) by a conventional photolithography method and then placed between PMMA film sheets (0.2 mm thick) using an adhesive bond (Super X, Cemedine Co., Ltd.). The films, including the parylene film, were inserted into the device to separate the wells (Figure S-1c and S-1d). Ag/AgCl electrodes of each device set into a solderless breadboard (E-CALL Enterprise Co., Ltd.) were connected to a Jet patch clamp amplifier (Tecella) using a jumper wire.<sup>32</sup> Two lipid monolayers were contacted together to prepare a stable and reproducible lipid bilayer in the parylene film (Figure S-1e). This method is advantageous for preparing model cell membranes; e.g., bacteria or mammalian cell membranes.

**pBLM Preparation and Reconstitution of Bombinins.** The pBLMs were prepared using an arrayed device, which had six chambers on the breadboard. Six individual lipid bilayers could be formed simultaneously in this device, which allowed for a higher-throughput measurement compared to the conventional system. First, the DOPE:DOPG = 3:1 mol mol<sup>-1</sup> (lipids/*n*-decane, 10 mg mL<sup>-1</sup>) solution (2.4 μL) was poured into all chambers. Next, the buffer solution (4.7 μL) with bombinin H2 or bombinin H4 or H2/H4 mix (1:1 mol mol<sup>-1</sup>) in 100 μM (final concentration) was poured into all chambers. In this study, the buffer solution (1 M KCl, 10 mM MOPS, pH 7.0) was used for all droplets. After a few minutes of adding the buffer solution, the two lipid monolayers connected and formed a lipid bilayer, and bombinin formed nanopores by reconstitution in the lipid bilayer. When the lipid bilayer ruptured, we reformed the lipid bilayer by tracing with a hydrophobic stick between two droplets.

**Channel Current Measurements and Data Analysis.** Channel current was monitored by using a JET patch clamp amplifier (Tecella) connected to each chamber. Ag/AgCl electrodes were in each droplet when we added the solution into the chambers. A constant voltage of +100 mV was applied to the one side, with the other side being grounded. The reconstituted bombinin pore in the lipid bilayers allowed ions to pass through the nanopore under the voltage gradient, so that we obtained the channel current signals. In our current measurement, we can find the single pore formation in the case of the step, multilevel, and spike signals: each step current corresponds to each pore formation the same as the case of pore-forming toxins (e.g., alpha-hemolysin), and the current rises up and returns to the baseline level, suggesting the single pore formation. These single pore formations are mostly observed in the initial stage of the current recordings. Because the lipid bilayer can be readily formed by using our droplet contact method,<sup>33</sup> we obtain a lot of single pore signals using our system. In the erratic signals, we cannot recognize the single pore formation because this signal can be assigned to the "carpet model" that is detergent like lipid dissociation. All measurements were conducted at room

temperature (ca. 23 °C) and analyzed as mean ± SE (*n* > 30). The signals were detected using a 4 kHz low-pass filter at a sampling frequency of 20 kHz. Analysis of channel current signals was performed using pCLAMP ver. 10.5 (Molecular Devices) and Excel (Microsoft) software.

**<sup>31</sup>P Solid-State NMR.** A total of 25 mg of bombinin peptide and dimyristoylphosphatidylcholine (DMPC) lipids with a peptide:lipid molar ratio = 1:10 was dissolved in the chloroform solvent and was evaporated. This was hydrated with 1 mL of Tris-NaCl buffer (20 mM, 100 mM NaCl, pH 7.5). A freeze-and-thaw cycle was repeated 10 times to form a multilamellar vesicle. <sup>31</sup>P solid-state NMR experiments were performed on a Chemagnetics CMX-400 infinity spectrometer equipped with a double resonance probe at the <sup>1</sup>H and <sup>31</sup>P resonance frequencies of 399.4 and 161.1 MHz, respectively. <sup>31</sup>P chemical shift values were referred to 85% H<sub>3</sub>PO<sub>4</sub> as 0.00 ppm (ppm). <sup>31</sup>P direct detection with high-power proton-decoupling static measurement was performed using 5.0 mm outer diameter at 30 °C for the fully hydrated samples.

**Cross-Linking Experiment.** Cross-linking reactions among the peptide-peptide in POPE/POPG lipid environments were performed by a BS<sup>3</sup> reagent which contains *N*-hydroxysulfosuccinimide (NHS) ester. The H2, [<sup>13</sup>C]Gly3-labeled H4, and the mixture of H2/the isotope-labeled H4 = 1:1 in POPE/POPG = 3:1 were mixed with BS<sup>3</sup> during short incubation for 30 min at 15 °C. After that, quenching buffer was added. In order to detect the cross-linked peptide as a dimer, above three kinds of the cross-linking product were recorded on MALDI-TOF MS (Bruker Daltonics, Autoflex speed TOF/TOF) equipped with a N<sub>2</sub> laser, respectively. All MS results were carefully obtained in the linear positive (LP) mode using α-cyano-4-hydroxycinnamic acid as a matrix.

## ASSOCIATED CONTENT

### Supporting Information

The Supporting Information is available free of charge on the ACS Publications website at DOI: 10.1021/acsabm.8b00835.

The device fabrications and detailed experimental data (PDF)

## AUTHOR INFORMATION

### Corresponding Author

\*E-mail: rjkawano@cc.tuat.ac.jp.

### ORCID

Izuru Kawamura: 0000-0002-8163-9695

Ryuji Kawano: 0000-0001-6523-0649

### Author Contributions

Y.S. and R.K. conceived the original idea and wrote the paper. Y.S., K.S., Y.K., and A.O. conducted the experiments and analyzed the data. R.K., Y.S., K.S., and I. K. wrote the paper. All authors have given approval to the final version of the manuscript.

### Author Contributions

||Equal contribution.

### Notes

The authors declare no competing financial interest.

## ACKNOWLEDGMENTS

This work was partly supported by KAKENHI (Grant No. 25708024, 15H00803, 16H06043, and 16H00828) from MEXT, Japan.

## REFERENCES

(1) Ollivaux, C.; Soye, D.; Toullec, J. Y. Biogenesis of D-Amino Acid Containing Peptides/Proteins: Where, When and How? *J. Pept. Sci.* 2014, 20 (8), 595–612.

- (2) Montecucchi, P. C.; Decastiglione, R.; Piani, S.; Gozzini, L.; Erspamer, V. Amino-Acid-Composition and Sequence of Dermorphin, a Novel Opiate-Like Peptide from the Skin of *Phyllomedusa-Sauvagei*. *Int. J. Pept. Protein Res.* **1981**, *17* (3), 275–283.
- (3) Mignogna, G.; Simmaco, M.; Kreil, G.; Barra, D. Antibacterial and Hemolytic Peptides Containing D-Alloisoleucine from the Skin of *Bombina-Variegata*. *EMBO J.* **1993**, *12* (12), 4829–4832.
- (4) Simmaco, M.; Kreil, G.; Barra, D. Bombinins, Antimicrobial Peptides from *Bombina* Species. *Biochim. Biophys. Acta, Biomembr.* **2009**, *1788* (8), 1551–1555.
- (5) Marr, A. K.; McGwire, B. S.; McMaster, W. R. Modes of Action of Leishmanicidal Antimicrobial Peptides. *Future Microbiol.* **2012**, *7* (9), 1047–1059.
- (6) Mangoni, M. L.; Papo, N.; Saugar, J. M.; Barra, D.; Shai, Y. C.; Simmaco, M.; Rivas, L. Effect of Natural L- to D-Amino Acid Conversion on the Organization, Membrane Binding, and Biological Function of the Antimicrobial Peptides Bombinins H. *Biochemistry* **2006**, *45* (13), 4266–4276.
- (7) Coccia, C.; Rinaldi, A. C.; Luca, V.; Barra, D.; Bozzi, A.; Di Giulio, A.; Veerman, E. C. I.; Mangoni, M. L. Membrane Interaction and Antibacterial Properties of Two Mildly Cationic Peptide Diastereomers, Bombinins H2 and H4, Isolated from *Bombina* Skin. *Eur. Biophys. J.* **2011**, *40* (4), 577–588.
- (8) Bozzi, A.; Mangoni, M. L.; Rinaldi, A. C.; Mignogna, G.; Aschi, M. Folding Propensity and Biological Activity of Peptides: The Effect of a Single Stereochemical Isomerization on the Conformational Properties of Bombinins in Aqueous Solution. *Biopolymers* **2008**, *89* (9), 769–778.
- (9) Montecucchi, P. C.; Decastiglione, R.; Piani, S.; Gozzini, L.; Erspamer, V. Amino-Acid-Composition and Sequence of Dermorphin, a Novel Opiate-Like Peptide from the Skin of *Phyllomedusa-Sauvagei*. *Int. J. Pept. Protein Res.* **1981**, *17* (3), 275–283, DOI: 10.1038/srep01995.
- (10) Hiratani, M.; Ohara, M.; Kawano, R. Amplification and Quantification of an Antisense Oligonucleotide from Target Microna Using Programmable DNA and a Biological Nanopore. *Anal. Chem.* **2017**, *89* (4), 2312–2317.
- (11) Ohara, M.; Takinoue, M.; Kawano, R. Nanopore Logic Operation with DNA to RNA Transcription in a Droplet System. *ACS Synth. Biol.* **2017**, *6* (7), 1427–1432.
- (12) Shoji, K.; Kawano, R. Microfluidic Formation of Double-Stacked Planar Bilayer Lipid Membranes by Controlling the Water-Oil Interface. *Micromachines* **2018**, *9* (5), 253.
- (13) Kawano, R. Nanopore Decoding of Oligonucleotides in DNA Computing. *Biotechnol. J.* **2018**, *13* (12), 1800091.
- (14) Watanabe, H.; Kawano, R. Channel Current Analysis for Pore-Forming Properties of an Antimicrobial Peptide, Magainin 1, Using the Droplet Contact Method. *Anal. Sci.* **2016**, *32* (1), 57–60.
- (15) Chui, J. K. W.; Fyles, T. M. Ionic Conductance of Synthetic Channels: Analysis, Lessons, and Recommendations. *Chem. Soc. Rev.* **2012**, *41* (1), 148–175.
- (16) Watanabe, H.; Gubbiotti, A.; Chinappi, M.; Takai, N.; Tanaka, K.; Tsumoto, K.; Kawano, R. Analysis of Pore Formation and Protein Translocation Using Large Biological Nanopores. *Anal. Chem.* **2017**, *89* (21), 11269–11277.
- (17) Yang, L.; Harroun, T. A.; Weiss, T. M.; Ding, L.; Huang, H. W. Barrel-Stave Model or Toroidal Model? A Case Study on Melittin Pores. *Biophys. J.* **2001**, *81* (3), 1475–1485.
- (18) Matsuzaki, K.; Murase, O.; Fujii, N.; Miyajima, K. An Antimicrobial Peptide, Magainin 2, Induced Rapid Flip-Flop of Phospholipids Coupled with Pore Formation and Peptide Translocation. *Biochemistry* **1996**, *35* (35), 11361–11368.
- (19) Pouny, Y.; Rapaport, D.; Mor, A.; Nicolas, P.; Shai, Y. Interaction of Antimicrobial Dermaseptin and Its Fluorescently Labeled Analogs with Phospholipid-Membranes. *Biochemistry* **1992**, *31* (49), 12416–12423.
- (20) Zasloff, M. Antimicrobial Peptides of Multicellular Organisms. *Nature* **2002**, *415* (6870), 389–395.
- (21) Nguyen, L. T.; Haney, E. F.; Vogel, H. J. The Expanding Scope of Antimicrobial Peptide Structures and Their Modes of Action. *Trends Biotechnol.* **2011**, *29* (9), 464–472.
- (22) Sekiya, Y.; Sakashita, S.; Shimizu, K.; Usui, K.; Kawano, R. Channel Current Analysis Estimates the Pore-Formation and the Penetration of Transmembrane Peptides. *Analyst* **2018**, *143* (15), 3540–3543.
- (23) Macazo, F. C.; White, R. J. Monitoring Charge Flux to Quantify Unusual Ligand-Induced Ion Channel Activity for Use in Biological Nanopore-Based Sensors. *Anal. Chem.* **2014**, *86* (11), 5519–5525.
- (24) Hille, B. *Ion Channels of Excitable Membranes*, 3rd ed.; Sinauer: Sunderland, Mass., 2001; p xviii, 814 p.
- (25) Gross, L. C. M.; Heron, A. J.; Baca, S. C.; Wallace, M. I. Determining Membrane Capacitance by Dynamic Control of Droplet Interface Bilayer Area. *Langmuir* **2011**, *27* (23), 14335–14342.
- (26) Mijiddorj, B.; Kaneda, S.; Sato, H.; Kitahashi, Y.; Javkhantugs, N.; Naito, A.; Ueda, K.; Kawamura, I. The Role of D-Allo-Isoleucine in the Deposition of the Anti-Leishmania Peptide Bombinin H4 as Revealed by <sup>31</sup>P Solid-State NMR, VCD Spectroscopy, and MD Simulation. *Biochim. Biophys. Acta, Proteins Proteomics* **2018**, *1866* (7), 789–798.
- (27) Zangger, K.; Gossler, R.; Khatai, L.; Lohner, K.; Jilek, A. Structures of the Glycine-Rich Diastereomeric Peptides Bombinin H2 and H4. *Toxicon* **2008**, *52* (2), 246–254.
- (28) Jilek, A.; Mollay, C.; Tippelt, C.; Grassi, J.; Mignogna, G.; Mullegger, J.; Sander, V.; Fehrer, C.; Barra, D.; Kreil, G. Biosynthesis of a D-Amino Acid in Peptide Linkage by an Enzyme from Frog Skin Secretions. *Proc. Natl. Acad. Sci. U. S. A.* **2005**, *102* (12), 4235–4239.
- (29) Kawano, R.; Horike, N.; Hijikata, Y.; Kondo, M.; Carne-Sanchez, A.; Larpent, P.; Ikemura, S.; Osaki, T.; Kamiya, K.; Kitagawa, S.; Takeuchi, S.; Furukawa, S. Metal-Organic Cuboctahedra for Synthetic Ion Channels with Multiple Conductance States. *Chem.* **2017**, *2* (3), 393–403.
- (30) Kawano, R. Synthetic Ion Channels and DNA Logic Gates as Components of Molecular Robots. *ChemPhysChem* **2018**, *19* (4), 359–366.
- (31) Norisada, K.; Javkhantugs, N.; Mishima, D.; Kawamura, I.; Saito, H.; Ueda, K.; Naito, A. Dynamic Structure and Orientation of Melittin Bound to Acidic Lipid Bilayers, as Revealed by Solid-State Nmr and Molecular Dynamics Simulation. *J. Phys. Chem. B* **2017**, *121* (8), 1802–1811.
- (32) Ohara, M.; Sekiya, Y.; Kawano, R. Hairpin DNA Unzipping Analysis Using a Biological Nanopore Array. *Electrochemistry* **2016**, *84* (5), 338–341.
- (33) Kawano, R.; Tsuji, Y.; Kamiya, K.; Kodama, T.; Osaki, T.; Miki, N.; Takeuchi, S. A Portable Lipid Bilayer System for Environmental Sensing with a Transmembrane Protein. *PLoS One* **2014**, *9* (7), No. e102427.